

Recent charm measurements through hadronic decay channels with STAR at RHIC in 200 GeV Cu+Cu collisions

Stephen Baumgart^a

Department of Physics, Yale University, 06520 New Haven, CT, USA

Received: 14 October 2008 / Revised: 7 March 2009 / Published online: 8 April 2009
© Springer-Verlag / Società Italiana di Fisica 2009

Abstract We report on the measurements of D^0 and D_s meson production in 200 GeV Cu+Cu collisions at the STAR at RHIC experiment. Results are discussed with reference to pQCD predictions of the open charm cross-section as well as the statistical hadronization model.

PACS 12.38.Mh · 21.65.Qr

1 Introduction

1.1 Charm production

The study of charm production has recently become an important sub-field of relativistic heavy ion physics. The large mass of the charm quark (between 1.2 and 1.8 GeV) allows one to calculate a total $c\bar{c}$ cross-section via pQCD [1]. Measurement of the charm spectra can provide insights into the new forms of matter generated in a relativistic heavy-ion collision. For example, a measurement of the nuclear modification factor, R_{AA} , which is the ratio of a particle's yield in A+A collisions divided by its yield in p+p collisions as a function of p_t and normalized by the number of binary collisions, can give insights into the properties of the medium as charm particles pass through it.

According to pQCD predictions $c\bar{c}$ pairs should be primarily produced through gluon fusion in the early stages of a relativistic heavy ion collision fireball at RHIC collision energies. The charm cross-section for 200 GeV nucleon on nucleon collisions can be calculated by summing Feynman diagrams at either the Next to Leading Order (NLO) or the Fixed Order Next to Leading Log (FONLL) levels [2]. Systematic error limits for the theoretical charm cross-section predictions are calculated by taking range of possible values of the charm quark mass and of the strong coupling constant.

Two alternate methods were used to predict the charm cross-section. In the first method, the differential cross-section was calculated for each p_t slice. These cross-sections were then integrated to achieve a final result of $\sigma_{c\bar{c}} = 244^{+381}_{-134} \mu\text{b}$ at the NL0 level and $\sigma_{c\bar{c}} = 256^{+400}_{-146} \mu\text{b}$ at the FONLL level [1]. The second method is to calculate the full charm cross-section over the full p_t range in one step. In this case charm cannot be treated as an active flavor (the charm quark is considered massive). The result obtained here is $\sigma_{c\bar{c}} = 310^{+1000}_{-210} \mu\text{b}$ [1]. Note the large error bar in the positive direction. This is due to the uncertainty in α_s when the momentum is roughly equal to the charm mass.

A measurement of a D^0 yield can be used to help find the charm cross-section. An extrapolation will have to be used to compute the $c\bar{c}$ yield from just the D^0 alone. Of course, a full measurement of the charm would require measuring all of the major charm hadrons ($D^0, D^{+/-}, D_s, \Lambda_c$). However, in STAR's Cu+Cu 200 GeV data, we have only been able to obtain the D^0 spectrum.

1.2 D_s production

A large enhancement of D_s meson production is expected in the presence of a quark-gluon plasma relative to a hadronic gas because D_s mesons become kinematically easier to produce during a deconfined phase. Assuming the plasma is thermalized, the statistical hadronization model can be used to predict the ratio of the D_s yield to other charmed mesons [3]. A measurement of the D_s yield can be used to either falsify or further verify the statistical hadronization model.

2 Procedure

2.1 Detectors

The analysis reported in this paper is based on data taken at the Solenoidal Tracker at RHIC (STAR) Experiment (see

^a e-mail: stephen.baumgart@yale.edu

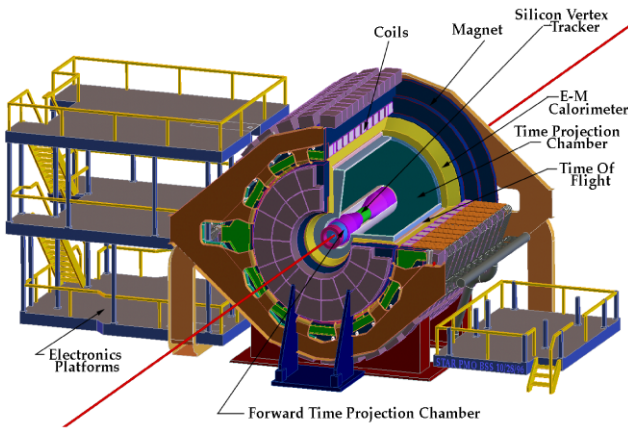


Fig. 1 The STAR detector

Fig. 1) at the Relativistic Heavy Ion Collider (RHIC). Both the D^0 and D_s analyses are based on data taken from STAR's Time Projection Chamber (TPC) [8]. The TPC is a gas-based tracking detector which completely surrounds the beam line in azimuth. Particles' momenta are calculated by using their curvature in a magnetic field. By measuring a particle's energy loss (dE/dx) as it transverses the TPC, particle identification can be done through use of the Bichsel parameterization [9].

The Silicon Vertex Tracker (SVT) [10] sits inside the TPC and can help identify charm mesons by finding their decay vertices. The SVT consists of three barrels of Silicon Drift Detectors which are used to reconstruct particle tracks to their origin. The SVT's vertex resolution is 60 μm , less than the D_s decay length of 149.9 μm .

2.2 Invariant mass reconstruction

By using the Bichsel parameterization method to do particle identification, lists of pion and kaon candidates and their associated momenta can be created. For some ranges of dE/dx and momenta pions and kaons are indistinguishable. In these cases, a single track can be listed as being both a pion candidate and a kaon candidate. In the region of dE/dx -momentum space where pions and kaons overlap, cuts on dE/dx and momentum are used to reduce the pion contamination of the kaons. Because there are so many more pions than kaons, cuts to reduce the kaon contamination of the pions are not necessary. The momenta are then used to reconstruct the invariant mass via the combinatorial technique. The D^0 (\bar{D}^0) is reconstructed through the $D^0 \rightarrow \pi^+ K^-$ ($\bar{D}^0 \rightarrow \pi^- K^+$) channel while the D_s^+ (D_s^-) is reconstructed through the $D_s^+ \rightarrow \phi \pi^+ \rightarrow K^+ K^- \pi^+$ ($D_s^- \rightarrow \phi \pi^- \rightarrow K^+ K^- \pi^-$). For the D^0 the formula is,

$$m_{D^0} = \sqrt{m_\pi^2 + m_K^2 + 2(E_\pi E_K - |p_\pi| |p_K| \cos(\theta))} \quad (1)$$

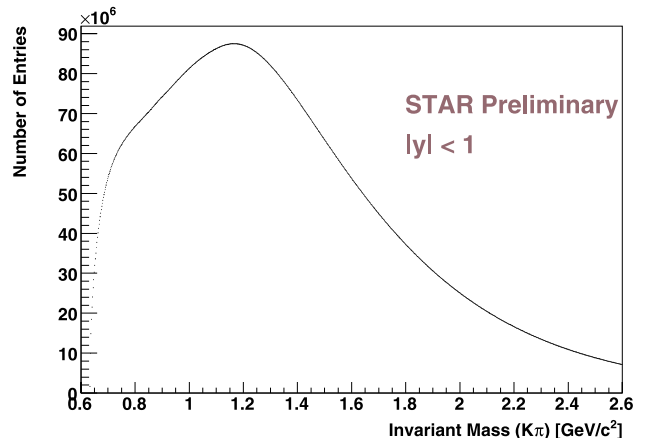


Fig. 2 The invariant mass distribution calculated from $K\pi$ combinations before background subtraction in 200 GeV Cu+Cu collisions

Here, θ is the angle between \vec{p}_π and \vec{p}_K . The D_s mass is calculated using a similar procedure. From here on D^0 will imply ' $D^0 + \bar{D}^0$ ' unless otherwise specified.

2.3 Background subtraction for the D^0

The D^0 mass peak is not visible before background subtraction (see Fig. 2). A simulation showed that the large slope of the underlying background would cause a Gaussian function the size of the D^0 peak to become invisible. Therefore, a background must be generated and subtracted. We do this using two different methods. In the first method the momentum vector of the kaon daughter of a D^0 candidate is rotated every 5 degrees between 150 and 210 degrees in the plane transverse to the beam line. This rotation destroys any resonance peaks. Multiple 5 degree rotations are used to reduce statistical noise in the background (this has been verified by simulation). However a rotational background subtraction does not eliminate any correlations coming from other resonances which may have misidentified daughters (for example, the K_s^0 has two pion daughters). If one pion is misidentified as a kaon the K^0 correlation will still remain after background subtraction. Another source of residual background is from collective flow. As with other misidentified resonances, since collective flow is a real physical correlation, it can not be subtracted using the rotational technique.

A second method of background subtraction is called 'event mixing'. In this case, kaon and pion tracks from different but similar events are used to reconstruct the background. Since it is impossible for tracks from different events to be correlated, this method should create a random background. However, events are always a little bit different in properties such as a total multiplicity, position, and reaction plane (this depends on the geometry of the colliding ions). Such differences may cause residual background to be created. Another concern is that event mixing does not conserve

total energy or momentum. Because of these factors, residual background remains.

In order to subtract the remaining residual background a polynomial curve is fit to the mass region around the D^0 peak after the event mixing or rotational background has been subtracted. The peak region itself is excluded from the fit. The polynomial function is then subtracted from the invariant mass spectrum to obtain the mass peak.

2.4 Reconstruction of the D_s meson

Though the D_s meson is also reconstructed through the invariant mass reconstruction technique, there are several important differences. Since the $c\tau$ of the D_s meson is 149.9 μm , a cut on the decay length can be used to improve the signal to background ratio. This requires the use of the SVT to trace back the daughter tracks of the D_s to the D_s decay vertex. Only tracks with decay lengths of between 100 μm and 500 μm are used to reconstruct D_s mesons. In order to dramatically reduce background, a cut on the intermediate ϕ resonance mass is made ($1.0145 \text{ GeV}/c^2 < m_{K^+K^-} < 1.0225 \text{ GeV}/c^2$). The ϕ resonance is visible before background subtraction. In order to approximately reconstruct the background, K^+K^- pairs away from the ϕ resonance are combined with π mesons to generate an invariant mass spectrum. Of course, the sample will also contain some true D_s mesons which do not decay through the ϕ resonance but their number is assumed to be negligible after the background is normalized to a region close to the D_s signal.

3 Results

3.1 D^0 yields

A D^0 signal was found with a significance of 4.3σ at mid-rapidity ($|y| < 1.0$) (see Fig. 3). The invariant mass spectrum was then split into three bins, one from 0.3 to $1.3 \text{ GeV}/c^2$, one from 1.3 to $2.3 \text{ GeV}/c^2$, and one from 2.3 to $4.3 \text{ GeV}/c^2$. The resulting yields were fit with an exponential in $m_t - m_0$ to obtain a yield via the formula

$$\frac{1}{2\pi N_{\text{events}}} \frac{d^2N}{p_t dp_t dy} = \left(\frac{dN_{D^0}}{dy} \right) \times \frac{e^{-(m_t - m_0)} T}{2\pi T(m_{D^0} + T)}. \quad (2)$$

The result of the fit is $\frac{dN_{D^0}}{dy} = 0.360 \pm 0.078(\text{stat.})$ (see Fig. 4). Since this is a mid-rapidity measurement of D^0 mesons, to convert to a full charm cross-section, an extrapolation must be made. This requires: (a) an extrapolation to full rapidity, (b) the ratio of D^0 to $c\bar{c}$, (c) a normalization to the number of binary collisions, and (d) a scaling to the inelastic cross-section of nucleons.

$$\sigma_{c\bar{c}}^{NN} = (dN_{D^0}/dy) \times (\sigma_{pp}^{\text{inelastic}} / N_{\text{bin}}^{\text{CuCu}}) \times (f/R). \quad (3)$$

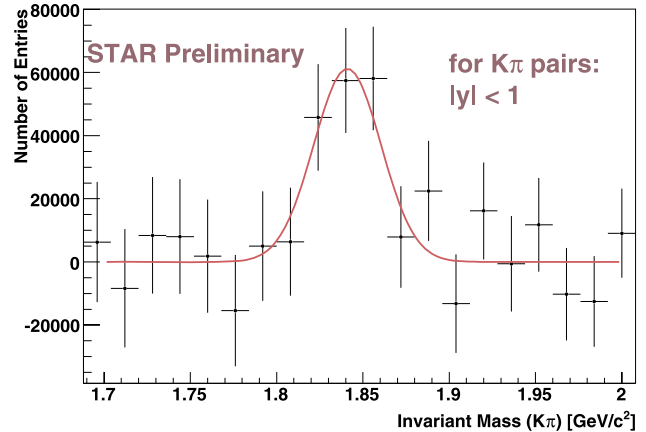


Fig. 3 $K^-\pi^+ + K^+\pi^-$ invariant mass spectrum after background subtraction in 200 GeV Cu+Cu collisions at 0–60% centrality after a residual background subtraction of a polynomial function

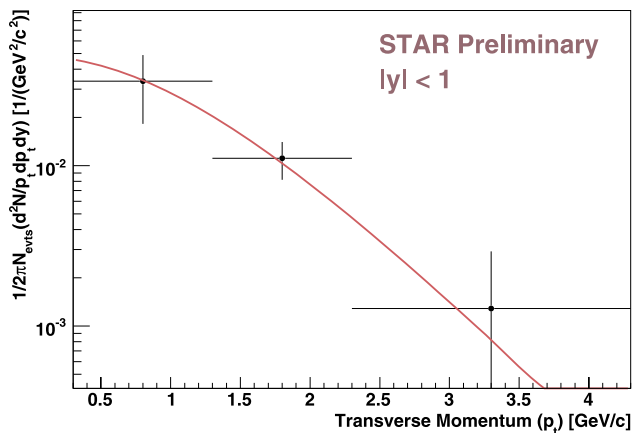


Fig. 4 The $D^0 + \bar{D}^0$ spectra in 200 GeV Cu+Cu collisions at 0–60% centrality fit with a decreasing exponential function

Where $f = 4.7 \pm 0.7$ is the normalization to full rapidity (calculated from simulation) [13], $R = 0.54 \pm 0.05$ is the ratio of D^0 to $c\bar{c}$ pairs as measured in e^+e^- collisions [11], $N_{\text{bin}}^{\text{CuCu}} = 80.4 + 5.9 - 5.6$ is the average number of binary collisions in a Cu+Cu collision with a centrality of 0 to 60%, and $\sigma_{pp}^{\text{inelastic}} = 42 \text{ mb}$ is the proton-proton inelastic cross-section [12]. After these factors are applied, the total charm cross-section in NN collisions is calculated to be $1.64 \pm 0.36(\text{stat.}) \text{ mb}$. Systematic error evaluation is still in progress.

3.2 D_s results

A candidate D_s^+ peak was found with a statistical significance of 3.0σ (see Fig. 5). This is too small of a significance to create a p_t spectrum. On the other hand, the possible detection of a peak is a good proof of principal that a D_s analysis based on inner silicon tracking can work. Strangely,

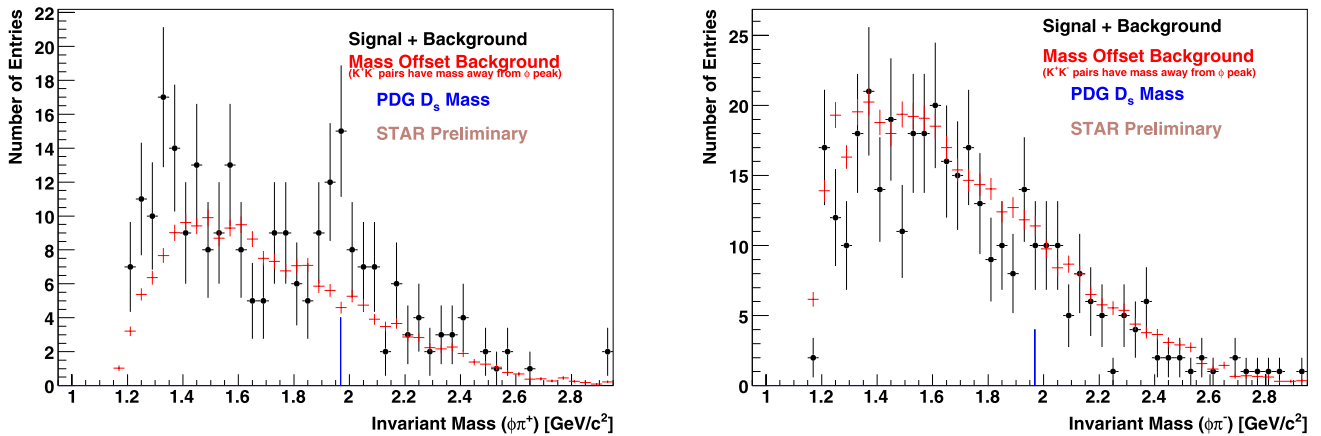


Fig. 5 (a) The $\phi\pi^+$ invariant mass spectrum. A candidate peak is visible near the D_s^+ mass. (b) The $\phi\pi^-$ invariant mass spectrum. No candidate peaks are visible

a D_s^+ population is seen but no D_s^- . This may either be due to low statistics or to a real physical effect. The raw yield of D_s^+ is 22 ± 11 counts. The upper limit of the raw D_s^- yield is 12 counts, assuming a statistical significance of 2 is needed in order to observe a signal, implying that the D_s^+ and D_s^- yields are still statistically consistent with a ratio of 1. Further measurements in 200 GeV d+Au and Au+Au collisions must be undertaken in order to fully understand whether the charge asymmetry is real.

4 Sources of systematic error

The systematic error evaluation is not yet complete but the sources of systematic error can be listed. Particle identification of tracks from the TPC through use of the Bichsel parameterization includes a systematic error. Also, the dE/dx-momentum cuts themselves are a source of systematic error. There is also a systematic error present from the choice of background subtraction (rotation or mixing).

5 Discussion

The measured Cu+Cu charm cross-section of 1.64 ± 0.36 (stat.) mb is consistent with previous STAR results assuming binary scaling (see Fig. 6) [6, 7]. This means that open charm is indeed produced during initial gluon fusion. However, the measured charm cross-sections are near the upper limit of the NLO prediction and far above the most probable theoretical prediction. This may have implications for the value of the charm mass and the strong coupling constant. The charm cross-section measured in 200 GeV Cu+Cu collisions, like other STAR measurements, is roughly a factor

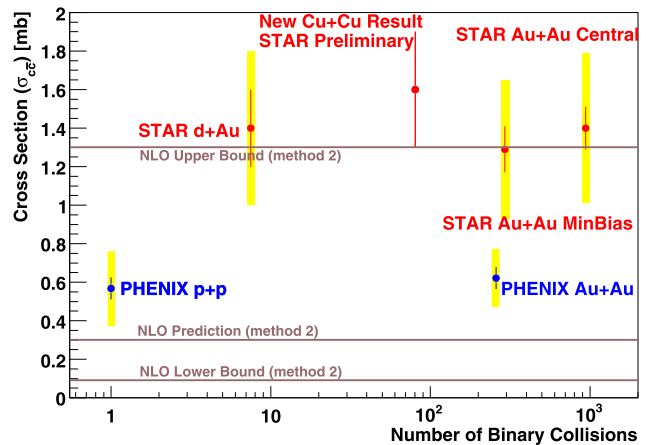


Fig. 6 The measured charm cross-sections of STAR and PHENIX [4–7]. NLO predictions are also marked out

of two larger than the mean of the charm cross-section measured by PHENIX. The cause of this discrepancy is still being investigated. Also, a candidate D_s^+ signal was found but no D_s^- . New measurements are needed to confirm whether this is a real physical effect or not.

References

1. R. Vogt, arxiv:hep-ph/0709.2531v1
2. M. Cacciari, P. Nason, R. Vogt, Phys. Rev. Lett. **95**, 122001 (2005)
3. I. Kuznetsova, J. Rafelski, Eur. Phys. J. C **51**, 113 (2007)
4. S.S. Adler et al. (PHENIX), Phys. Rev. Lett. **94**, 082301 (2005)
5. S.S. Adler et al. (PHENIX), Phys. Rev. Lett. **97**, 252002 (2005)
6. J. Adam et al. (STAR), Phys. Rev. Lett. **94**, 062301 (2005)
7. B.I. Abelev et al. (STAR), arxiv:nucl-ex/0805.0364
8. M. Anderson et al. (STAR TPC Group), Nucl. Instrum. Methods A **499**, 659 (2003)
9. H. Bichsel, Nucl. Instrum. Methods A **562**, 154 (2006)

10. R. Bellwied et al. (STAR SVT Group), Nucl. Instrum. Methods A **499**, 640 (2003)
11. W.-M. Yao et al. (Particle Data Group), J. Phys. G: Nucl. Part. Phys. **33**, 1 (2006)
12. S.S. Adler et al. (STAR), Phys. Rev. Lett. **91**, 172302 (2003)
13. T. Shöstrand et al., Comput. Phys. Commun. **135**, 238. PYTHIA 6.152, MSEL = 1, CTEQ5M1